EXPERIMENTAL STUDY OF SYNTHETIC JETS WITH RECTANGULAR ORIFICE

Fernanda Munhoz
Conrad Yuan Yuen Lee
Universidade do Vale do Rio dos Sinos - UNISINOS
Av. Unisinos, 950 - São Leopoldo, RS, Brasil CEP 93022-000
fe2506@yahoo.com.br; conrady@unisinos.br

Franciele Laura Dutra Alves
Universidade do Vale do Rio dos Sinos - UNISINOS
Av. Unisinos, 950 - São Leopoldo, RS, Brasil CEP 93022-000
francielealves@yahoo.com.br

Abstract. Modern electronics are becoming more compact and with higher processing power, which translates into a demand for higher heat dissipation. Current electronic "coolers," which are based on the combination of fans and heat sinks, are becoming unable to provide sufficient heat dissipation since they rely primarily on moving large volumes of air to achieve their results. As an alternative, synthetic jets are under consideration due to their known property to enhance heat transfer. Synthetic jets are produced by the oscillation of a membrane in a sealed cavity equipped with an orifice. For this study, a numerical model of channel mounted with a heating element on one surface and a synthetic jet directed to blow along the wall constructed on ANSYS CFX with the SST k-ω turbulence model. Heat dissipation provided by the synthetic jet was analyzed with changes to the Reynolds number, pulsing frequency and placement of the heated element. Results were compared to a conventional technique represented by a steady channel flow of equivalent mass flow rate to the average flow induced by the synthetic jet. Results confirm that the synthetic jet greatly outperforms the conventional channel flow and suggest the need for further studies in this area.

Keywords: synthetic jets; Reynolds number; electronic cooling devices.

1. INTRODUCTION

Overheating is the primary causes of failure in electronic devices. Consequently, new and more efficient forms of heat dissipation are needed to cope with the rising cooling demand (CHAUDHARI *et al.*, 2010). Even as electronic components become more compact, a temperature below 85 °C or lower is still needed to ensure its operation (BHOWMIK *et al.*, 2005, MATHEWS AND BALAJI, 2006). Moreover, the constant advance in electronic design results in higher core densities which increase the amount of power being consumed and heat generation. All this stresses the need for more efficient heat transfer techniques capable of maintaining the devices operating within their specified safety range (CHANDRATILLEKE *et al.*, 2010, KALTEH *et al.*, 2011). New heat dissipation techniques, such as microchannels, micro heat pipes, thermoelectric coolers, or liquid cold plates have been considered to address the problem (ETEMOGLU, 2007).

As noted by Xu *et al.* (1998), air is widely used as the working fluid in electronic cooling due to its negligible cost and availability. However, it was also noted that, for higher heat dissipation demands, liquid cooling is more readily able to handle the temperatures of high power systems. Despite this fact, forced air convection still remains the least expensive and more reliable form of cooling. The downside of forced air convection, as observed by Chaudhari *et al.* (2010a, 2010b), is the need to provide a large volume of air to create a pressure difference sufficient to flow through the narrow network of channels and fins that make up a heat sink. Therefore any technique that can enhance heat transfer for the current amount of airflow available is worthy of study (OHADI, 2003). This, synthetic jets are viewed with great interest due to their known capability to enhance mixing or achieve turbulence control. In particular, synthetic jets the lack the need for an external source of fluid and have the potential for miniaturization, which allow the fabrication of such devices embedded directly alongside the electronic components.

Most cooling studies with synthetic jets make use of a direct impact configuration, in which the synthetic jet actuator is placed facing a heated surface and the jet collides directly with the heating element. However, Mahalingan e Glezer (2005) opted to use a different configuration in which the synthetic jet is directed to blow alongside one of the walls of a channel representing the surface of a fin. Under continuous operation, the effect of the synthetic jet was to induce a mean flow through the channel. Experimental results show that the convective heat transfer coefficient of the synthetic jet was 150% higher than for a conventional steady channel flow of equivalent mean mass flow rate. Thus, this study seeks to gain further understanding on the cooling performance of this configuration. Since the study is conducted numerically, parametric studies on the effect of pulsing frequency, Reynolds number, and placement of the heated surface are conducted looking to categorize their effect on the convective heat transfer coefficient and Nusselt number.

ISSN 2176-5480

Marcos Leandro Woyciekoski, Conrad Yuan Yuen Lee and Jacqueline Biancon Copetti
Experimental Study Of Synthetic Jets With Rectangular Orifice

(single space line, size 10)
2. SYNTHETIC JETS
(single space line, size 10)

A synthetic jet is formed when fluid is alternately expelled and drawn into a cavity. The usual configuration of a synthetic jet actuator consists of a cavity sealed on end with a flexible membrane and on the other end with a plate in which an orifice is cut out (GLEZER *et al.*, 2003). Figure 1 shows a schematic of a synthetic jet generator and the ensuing jet. As it can be seen on Fig. 1, a synthetic jet actuator does not require an external source of fluid, such as a feed tank of pressurized air, since the same fluid in external region also fills the cavity (GLEZER *et al.*, 2003). Thus it is a zero-mass-flux or zero-net-mass-flux device (WANG *et al.*, 2010). However, despite the zero mass flow balance of fluid in and out of the cavity, a net positive momentum develops in the external region with characteristics similar to a steady jet (CHAUDHARI *et al.*, 2010; JAIN *et al.*, 2011).
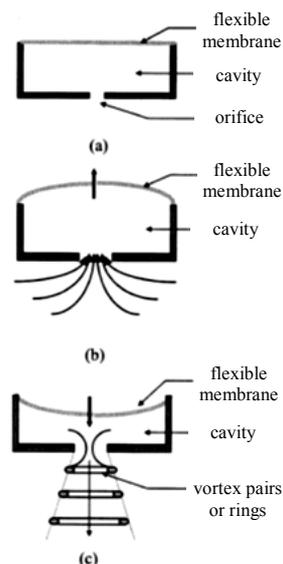

Figure 1. Schematic of a synthetic jet actuator and its operation: (a) basic components; (b) suctioning phase; (c) ejection phase and formation of synthetic jet.
Source: Adapted from Glezer *et. al*, (2003).

In a synthetic jet actuator, the cavity is initially filled with the same fluid as the external region. Periodic oscillations in the cavity volume expel fluid forming a jet in the external region (TANG et al., 2009). This oscillation can be achieved with several driving mechanism, such as electrostatic, electromagnetic or piezoelectric pistons, membranes or diaphragms. Piezoelectric actuators have the advantage of lightness and low power consumption while electromagnetic actuators are more silent and durable (WILLIAMS *et al.*, 2007). While the physical scale of synthetic jet actuators may vary, micro-fabrication techniques make them ideal for direct integration alongside electronic components with relatively low cost (CHAUDHARI *et al.*, 2010).

The synthetic jet is formed during the ejection phase of the actuator, as fluid rolls up on the shear layer at the edge of the orifice to form a vortex pair or ring. This vorticity is the driving mechanism behind the enhanced convection and turbulence caused by the jet. While the production of vorticity also occurs on steady jets, the oscillatory nature of the synthetic jet augments this phenomenon considerably. For the correct operation of a synthetic jet, the ejected vorticity must contain sufficient celerity so that it is not re-ingested into the cavity when the actuator reverses direction. If these conditions are met, the cavity is filled during the suction phase by fluid from the external medium drawn in along the sides of the orifice (WILLIAMS *et al.*, 2007).

Chaudhari *et al*. (2008) analyzed the effect of pulsing frequency on the ensuing jet for different cavity depths and orifice diameters. Results show that the synthetic jet reached a substantial velocity range within a narrow frequency range. Moreover, 2 critical frequencies were identified within this frequency range at which the velocity peaked. These values were identified as the resonant frequency of the diaphragm and the Helmholtz frequency of the cavity. The resonant frequency of the diaphragm can be calculated based on its geometry and elastic properties of the assembly. In comparison, the Helmholtz frequency is obtained through the solution of the Helmholtz equation and takes in consideration geometric factors in the cavity and orifice as well as material and acoustic properties of the working fluid. Other relevant results from Chaudhari *et al*. (2008) noted that the operating frequency range became narrower with increasing orifice diameter and the cavity depth has a more pronounced effect only for smaller orifice diameters and at the Helmholtz frequency.

2.1 Physical Flow Parameters

The main parameters of interest for this study are the Strouhal number, Reynolds number and Nusselt number. The Strouhal number (St_{U0}) is used to characterize oscillating flows, where it functions as a dimensionless measure of frequency. Its application in synthetic jets is to serve as a limiting actuation value, above which no synthetic jet is issued from the orifice. The mathematical expression of St_{U0} used in this study is given by (1):

$$St_{U0} = \frac{2\pi fH}{U_0} \tag{1}$$

where f is the pulsing frequency of the jet, H is the orifice diameter and U_0 is the average exit jet velocity defined according to (2):

$$U_0 = \frac{L_0}{\tau} \tag{2}$$

where τ is the period of oscillation ($1/f$) and L_0 is the average column of fluid ejected during the blowing phase of actuation defined as (3):

$$L_0 = \int_0^{\tau/2} u_0(t)dt \tag{3}$$

where $u_0(t)$ is the time-varying mean velocity across the orifice exit plane.

The Reynolds number (Re) is defined according to the average jet velocity in order to characterize the performance ot eh synthetic jet, being defined as (4):

$$Re = \frac{\rho U_0 H}{\mu} \tag{4}$$

where ρ is the density and μ the dynamic viscosity of the fluid.

For problems relating to heat transfer, the local Nussel number (Nu_h) becomes an important analysis parameter, being defined in this study as (5):

$$Nu_h = \frac{hd^*}{k} \tag{5}$$

where h is the convective heat transfer coefficient, d^* is a characteristic length of the surface and k is the thermal conductivity of the fluid.

3. METHODOLOGY

This study applies CFD in order to conduct a parametric study on geometric and flow parameters affecting the heat transfer obtained by a synthetic jet blown alongside a surface containing a heating element.

3.1 Numerical Model

The numerical model is implemented through ANSYS CFX 12.0, which makes use of a control volume approach to solve the Reynolds-averaged Navier-Stokes and energy equations. The control volume approach approximates each term in the governing equations with a finite difference written from the conservation of mass, momentum and energy around each element in the computational mesh (MALISCA, 2004). Thus, the precision of this approach is sensitive to the number elements in the computational mesh. For a turbulent flow, additional turbulence model equations are needed to properly account for the effects induced by the channel walls and, due to the small scale of these phenomena, the mesh needs to be locally more refined than in other regions of the domain. The amount of refinement depends on the turbulence model being considered. For the traditional k-ε model at low channel Reynolds numbers, grid resolutions near the wall of $y^+<2$ (wall units) are needed (ANSYS, 2009). A similar grid resolution is needed for the *SST k-ω* model. However, this model, which applies a k-ε model at regions away from the surface and a k-ω model near the surface, is considered to provide more accurate results on the flow-wall interactions.

3.2 Domain Geometry

The geometry studied consists of a 2-D channel filled with fluid as seen on Figure 2. The lower surface is defined as a no-slip wall, while the left and right borders are defined as openings at the same static pressure and initially with no mass flow. The top surface is defined as a symmetry condition, so that the computational domain is essentially the bottom half of a symmetric design. A thin plate is placed at a height H above the lower surface to form the throat for the synthetic jet actuator. The throat length was made to be excessively long, at least $25H$ so that jet formation would not be affected by the pressure condition at the left opening. The long throat length also precludes the need to simulate the cavity and membrane parts of the synthetic jet actuator. While experimental studies such as Chaudhari *et al*. (2008) noted the effect of cavity depth on the ensuing jet, the long throat length used in this study tends to cancel out such effects and the exiting jet velocity profile resembles a fully developed channel flow. Thus, in the absence of a cavity and membrane, a time-varying velocity profile is applied directly at the throat inlet and the flow is allowed to develop naturally along its length. Based on the orifice diameter H, the channel has an overall length of $200H$ and height of $9,5H$.
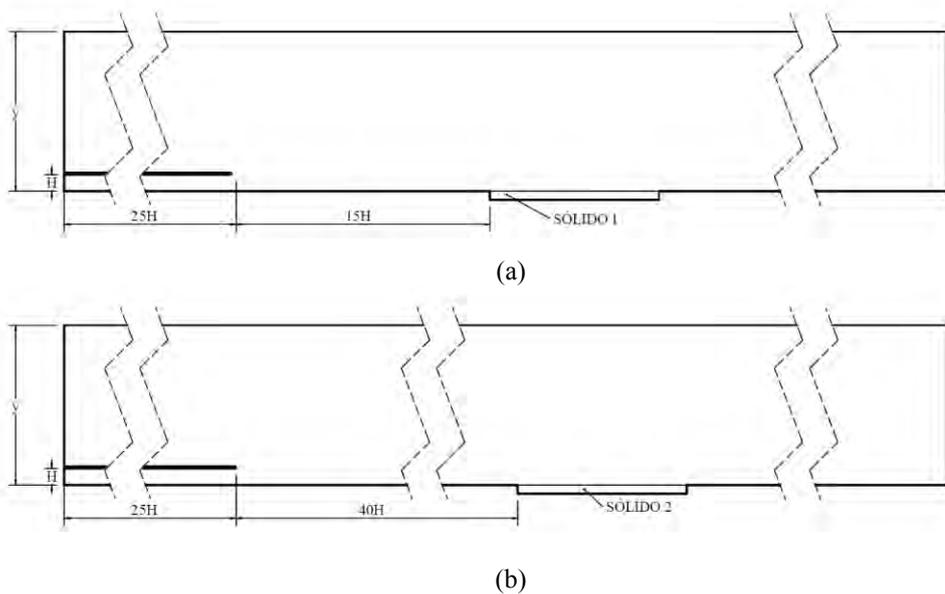

(a)

(b)

Figure 2. Schematic of channel geometries used in this study: (a) Solid 1 and (b) Solid .

For the heat transfer analysis, a heated element representing an electronic chip measuring $10H$ in length and a depth of $0,5H$ is embedded on the lower surface. As seen on figure 2, two locations for the electronic chip are considered based on the distance between the jet orifice exit plane and the start of the heated region: Solid 1(Fig. 2(a)) has a distance of $15H$ while Solid 2 (Fig. 2(b)) has a distance of $40H$. In addition to vertical grid refinement near the wall, selective horizontal grid refinement is also applied at regions where higher gradients are expected to occur, or where additional resolution is deemed beneficial, as seen on Figure 3. These regions are identified to be around the jet orifice exit plane (Fig. 3(a)) and upstream and downstream of the heated region (Fig. 3(b)). Overall, the computational meshes used in this study contain around 90.000 elements and 180.000 nodes.
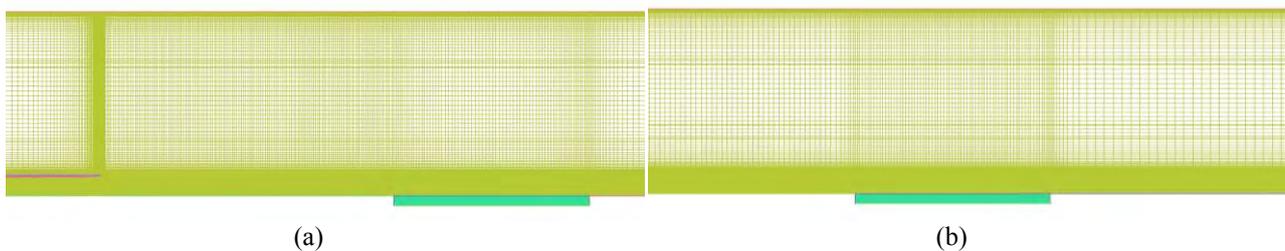

(a)   (b)

Figure 3. Sample grid refinement: (a) at jet orifice exit region and (b) around heated region.

3.3 Validation of Channel Geometry

The current grid and numerical method was tested with the computational domain without the raised plate that forms the jet throat. Thus the geometry was essentially that of an channel flow. A pressure gradient was specified

between the left and right openings and the resulting flow allowed to develop until a steady state condition is reached. The jet profile near channel exit was extracted and the result compared to the universal turbulent boundary layer profile of White (1991). The extracted velocity was found to be well matched to the theoretical profile, containing all expected regions: laminar sublayer, overlap region and log-law region. The resulting mass flow rate is applied as a boundary condition and the resulting pressure gradient and developed velocity profile were found to be the same as the initial test. This mesh resolution was kept throughout the remainder of this study and since all other simulations resulted in average flow rates much inferior to the one used in the validation cases, the computational mesh was deemed to be sufficient to obtain accurate results of the resulting turbulent structures.

3.4 Initial Conditions and Test Parameters

As mentioned in section 3.1, in lieu of simulating a cavity and membrane, a velocity profile is imposed at the inlet plane of the jet throat. This velocity profile has a sinusoidal shape and sinusoidal time variation as shown by (6):

$$u(y,t) = A_0 \sin\left(\frac{2\pi t}{\tau}\right) \sin\left(\frac{\pi y}{H}\right) \tag{6}$$

where A_0 is the amplitude of velocity oscillation, y is the spanwise distance and t is time. The amplitude A_0 is defined so that the time varying mean velocity $u_0(t)$ in (3) results in a U_0 half of the value used in the turbulent jet of Smith and Glezer (1998). For this case, an A_0=0,755 m/s is found to result in a Re=172. From this baseline case, the amplitudes of velocity corresponding to $(1/2) A_0$ and $(3/2) A_0$ are also examined. The range of Re tested in this study are shown on Table 1.

Table 1. Variation in jet velocity amplitude and resulting average exit jet velocity (U_0) and Reynolds numbers (Re).

Amplitude	U_0 [m/s]	Re
$0,5A_0$	0,077	85,8
$1,0A_0^{(1)}$	0,153	172
$1,5A_0$	0,230	257

[(1)]: baseline value of 0,755 m/s

Two values of pulsing frequency (f) are also considered, of 1 Hz (case 1St) and 0,5 Hz (case 2St), selected in order to reduce the computational time needed to complete the parametric study. These values are considerably lower than experimental studies but their resulting St_{U0} values are below the minimum value needed to induce the formation of vorticity. Consequently, they are considered sufficient to obtain a measure of the effect of pulsing frequency on jet cooling. The range of St_{U0} tested is shown on Table 2:

Table 2. Strouhal numbers (St_{U0}) for each pulsing frequency (f) and Reynolds number (Re)

Re	1St (1 Hz)	2St (0,5 Hz)
85,8	0,082	0,164
172	0,041	0,082
257	0,027	0,055

The variations in Re and St_{U0} are applied to both Solid 1 and Solid 2 configurations, so that in all, 12 separate cases are examined in this study. Initial conditions consisted of fluid at rest in the channel at a uniform temperature of 290 K. At the start of jet actuation, a temperature of 300 K is applied uniformly along the embedded bottom of the heating element and heat allowed to flow through the solid region and into the solid. The fluid and solid elements were defined so that the thermal conductivity of the solid is 690 times greater than the fluid. As fluid flows through the left and right openings of the channel, new fluid that is drawn in is also assumed to be at 290 K.

Each synthetic jet case is allowed to go through 10 pulsing cycles, at which point the time average velocity and temperature fields were calculated. For comparison purposes, an additional run is tested in which the calculated mean mass flow rate is applied as a left side inlet condition with the synthetic jet turned off in order to obtain a conventional, steady flow on a channel with a backwards-facing step.

4. RESULTS

Each synthetic jet case is compared to its respective steady channel with backwards-facing step version. Thus a direct comparison can be made between the heat dissipation produced by the synthetic jet and a conventional flow in

Marcos Leandro Woyciekoski, Conrad Yuan Yuen Lee and Jacqueline Biancon Copetti
Experimental Study Of Synthetic Jets With Rectangular Orifice

which a large single fan drives a steady volume of air through a heat sink. For each case, the convective heat transfer coefficient averaged over the heated surface and local Nu_h is calculated taking the characteristic length d^* to be the length of the heated region along the plate. Results are shown on Table 3(a) for both Solid configurations and *1St* case and Table 4for both Solid configurations and the *2St* case. The columns labeled "Synth. jet" displays the values obtained with the synthetic jet actuator while the columns labeled "Steady" are the corresponding conventional steady flow through the channel.

Table 3(a). Heat transfer results for Solid 1 and *1St* case.

Re	h [W/(m²K)]		Nu_h	
	Synth. jet	Steady	Synth. jet	Steady
85,8	1830	960	30,2	15,8
172	3730	2070	61,5	34,0
257	9610	4350	158	71,7

Table 3(b). Heat transfer results for Solid 2 and *1St* case.

Re	h [W/(m²K)]		Nu_h	
	Synth. jet	Steady	Synth. jet	Steady
85,8	1450	1020	23,9	16,8
172	3460	2217	57,0	36,8
257	9520	4280	157	70,5

Table 4(a). Heat transfer results for Solid 1 and *2St* case.

Re	h [W/(m²K)]		Nu_h	
	Synth. jet	Steady	Synth. jet	Steady
85,8	1690	903,5	27,9	15,0
172	3580	2020	59,0	33,3
257	8940	4280	147	70,5

Table 4(b). Heat transfer results for Solid 2 and *2St* case.

Re	h [W/(m²K)]		Nu_h	
	Synth. jet	Steady	Synth. jet	Steady
85,8	1440	921	23,8	15,2
172	3490	2150	57,6	35,4
257	8950	4190	148	69,0

Tables 3 and 4 show that synthetic jet-driven cooling outperforms the conventional steady channel flow for every single combination of *Re*, St_{U0} and placement of the heated region. Overall, for the Solid 1 configuration and *1St* case (Table 3(a)), h and Nu_h gains for the synthetic jet over the conventional channel flow ranged from 90% to 120%. For the same configuration but decreasing the pulsing frequency to the *2St* case (Table 4(a)), the relative gains were similar, from 85% to 108%. Changing the placement of the heated region to the Solid 2 configuration, results show a gain ranging from 42% to 123% for the *1St* case (Table 3(b)) and from 57% to 115% for the *2St* case (Table 4(b)). These results are within the experimental results of Mahalingan and Glezer (2005), which reported gains as high as 150% in thermal performance. The difference in performance in this study may be explained by the 2-D geometry and the fact that the current geometry limits the heated region to a small region of the channel while the experiment of Mahalingan and Glezer (2005) presented the entire bottom surface as heated.

Parametric variation shows that heat transfer tends to increase with increasing *Re*. The gains themselves are not exactly proportional. Starting from an *Re* of 85,8 and doubling its value to 172 results in increases in h and Nu_h in factors ranging from 2 to 2,8. If this initial *Re* is increased by a factor of 3 to 257, h and Nu_h increase in factors ranging from 5,2 to 6,2. These gains occur to both the synthetic jet-driven cooling and the conventional steady channel flow. Looking only at the effect of geometric parameters on synthetic jet cooling, when the heated region is placed nearer to the jet exit orifice, the resulting values of h and Nu_h are found to be higher for both pulsing frequencies. The effect of pulsing frequency also becomes more distinct when the heated region is placed closer to the jet exit orifice. In this case, such as for the results of Solid 1 on Table 3(a) and Table 4(a), higher frequencies result in slightly higher heat transfer.

When the heated region is placed further away as in Solid 2, there is little variation in heat transfer with pulsing frequency as seen on Table 3(b) and Table 4(b).

Further observations can be drawn by presenting the data from Tables 3 and 4 in graphical form, shown on Figures 4 and 5. Figure 4 shows the variation of Nu_h with Re for both Solid configurations and $1St$ case while Figure 5 shows the same plot but for the $2St$ case. As noted previously, both the synthetic jet and conventional steady channel flow present increasing Nu_h with Re. However Fig. 5 and 6 clearly show that the Nu_h growth for the synthetic jet is steeper. Placement of the heated region presented very little effect on the conventional channel flow, with Nu_h points essentially overlapping along the bottom of each graph. A similar situation occurs for the synthetic jet, except for then when the heated region is placed near the exit point of the jet, and the pulsing frequency is higher.
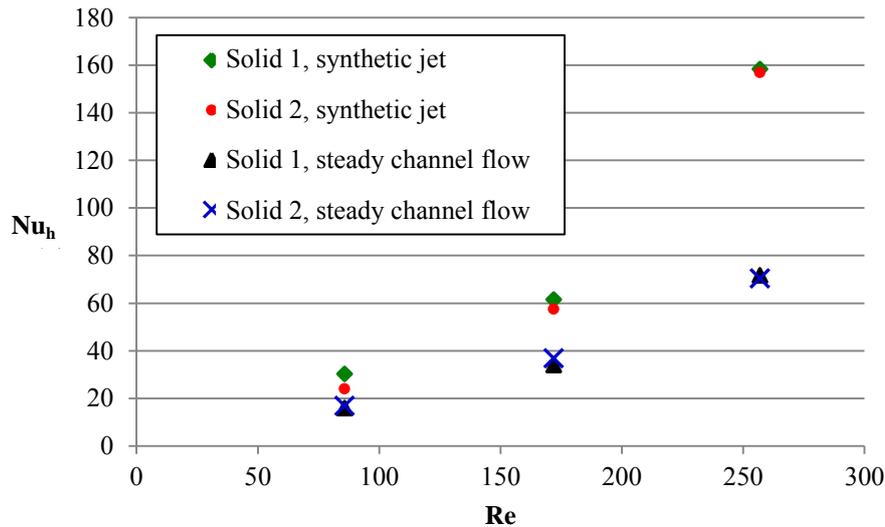

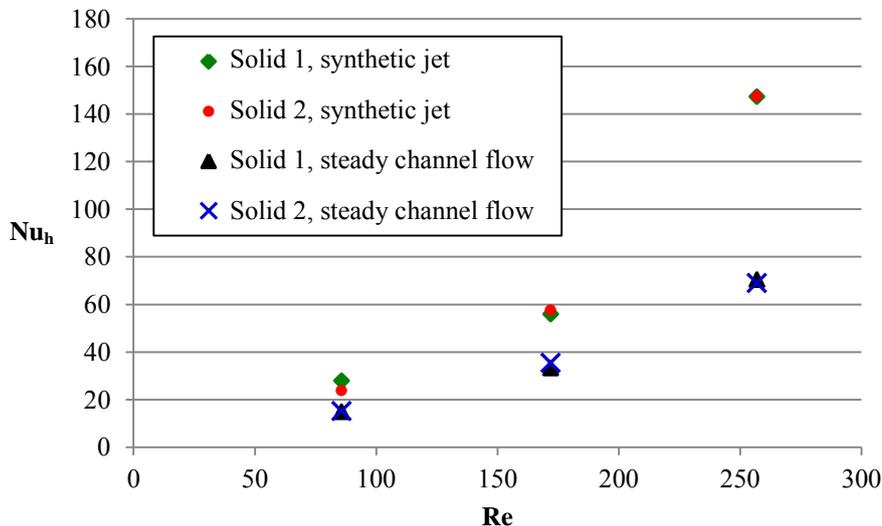Figure 4. Nu_h vs. Re for both Solid configurations and $1St$ case.

Figure 5. Nu_h vs. Re for both Solid configurations and $2St$ case.

The superior cooling performance of the synthetic jet can be visually confirmed through the normalized contours of the absolute average vorticity shown on Figure 6. Data for Fig. 6 is for the baseline $Re=172$ and $ST_{U0}=0,041$ averaged over the 10th pulsing cycle. For each Solid configuration, the equivalent conventional steady channel flow is also shown for comparison purposes. It can be seen on Fig. 6(a) and (c) for the synthetic jet that fluid feeding the jet is drawn from the left opening, dragged along the outside of the jet throat and rolled on the orifice edge as it is suctioned into the throat. Meanwhile, ejected flow is blown downstream and flows the length of the channel in a layer of thickening vorticity. In contrast, the conventional steady channel flow (Fig. 6(b) and (d)) shows a typical backwards-facing step

Marcos Leandro Woyciekoski, Conrad Yuan Yuen Lee and Jacqueline Biancon Copetti
Experimental Study Of Synthetic Jets With Rectangular Orifice

flow with fluid separation occurring at the edge of the step and reattachment occurring approximately at the Solid 1 position. Since all contours are plotted on the same scale, it can be clearly seen that the synthetic jet-driven flow generates substantially more vorticity than the steady conventional flow. Since vorticity near the wall is associated with the presence of turbulence phenomena, the resulting increase on flow mixing results in the calculated improvements on h and Nu_h.
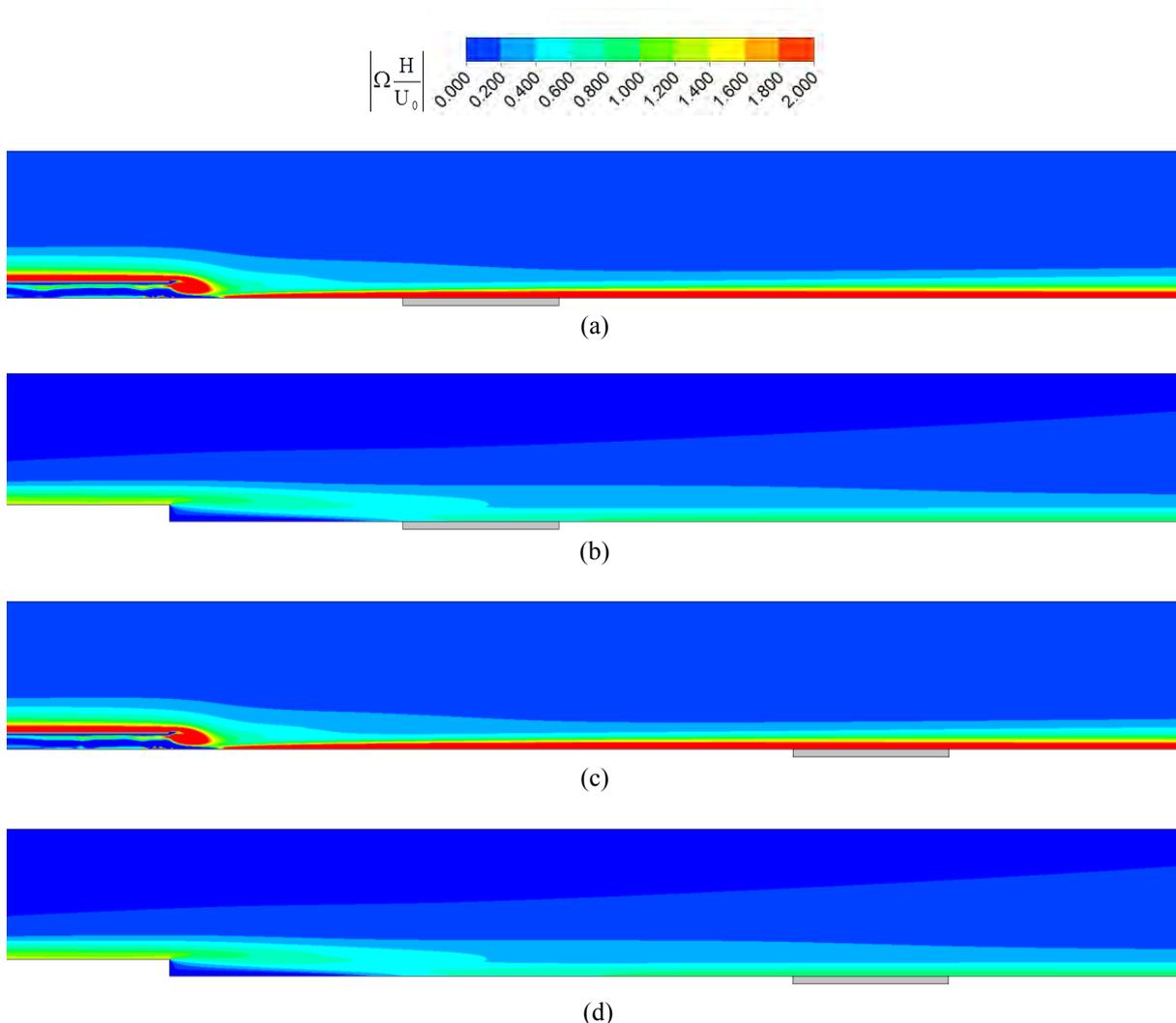

(a)

(b)

(c)

(d)

Figure 6. Time-averaged normalized absolute vorticity contours ($Re = 172$, $St_{U0} = 0,041$) for (a) Solid 1 over the 10th pulsing cycle; (b) Solid 1 with steady channel flow; (c) Solid 2 over the 10th pulsing cycle; (d) Solid 2 with steady channel flow.

5. CONCLUSIONS

A cooling problem in which a synthetic jet is directed to blow along the wall of a channel containing a heating element is examined in this study. Results show that synthetic jet-driven channel flows greatly outperform conventional steady channel flows of equivalent average mass flow rate. Improvements in convective heat transfer coefficient and Nusselt number are determined to range from as low as 42% and as high as 123%, which are comparable to experimental data. Parametric studies confirm that the improvement in cooling performance increases with jet Reynolds number. Placement of the heated region closer to the exit jet plane also yields improved performance. While in general, pulsing frequency is a relevant parameter for synthetic jets, for this particular geometric configuration its effect is felt mainly when the heating element is placed closer to the exit jet plane. Closer examination of the average vorticity field confirms that the improved cooling performance of the synthetic jet-driven flow is a result of the substantial amount of vorticity generated along the wall due to flow oscillations induced by the jet. Results show that synthetic jets are a viable replacement method to conventional forced convection techniques and further studies are needed to examine the effect of other geometric and flow parameters not examined in this study.

6. ACKNOWLEDGEMENTS

7. REFERENCES

ANSYS CFX, 2009, "Ansys CFX-Solver modeling Guide", Release 12.0.

Chandratilleke, T. T., Jagannatha, D. e Narayanaswamy, R., 2010, "Heat Transfer Enhancement in Microchannels With Cross-Flow Synthetic Jets", International Journal of Thermal Sciences, V. 49, N. 3, p. 504-513.

Chaudhari, M., Puranik, B. e Agrawal, A., 2010a, "Heat Transfer Characteristcs of Synthetic Jet Impingement Cooling", International Journal of Heat and Mass Transfer, V. 53, p. 1057-1069.

Chaudhari, M., Puranik, B. e Agrawal, A., 2010b, "Effect of Orifice Shape in Synthetic Jet Based Impingement Cooling", Experimental Thermal and Fluid Science, V. 34, p. 246-256.

Chaudhari, M.,Verma G., Puranik, B. and Agrawal, A., 2009, "Frequency response of a synthetic jet orifice," Exp. Thermal and Fluid Sci. V. 33, p. 439-448.

Glezer, A., Allen, M. G., Brand, O., Lee, J. B. e Kercher D. S., 2003, "Microjet Cooling Devices for Thermal Management of Eletronics", IEEE Transactions on Components and Packaging Technologies, V. 26, N. 2, p. 359-366.

Jain, M., Puranik, B. e Agrawal, A., 2011, "A Numerical Investigation of Effects of Cavity and Orifice Parameters on Characteristics of a Synthetic Jet Flow Department of Mechanical Engineering", Indian Institute of Technology Bombay, Powai, Mumbai 400076, India.

Kalteh, M., Abbassi, A., Agrawal, A., Saffar-Avval, M., Frijns, A., Darhuber, A. e Harting J., 2011, "Experimental and Numeral Invetigation of Nanofluid Forced Convection Inside a Wide Microchannel Heat Sink", Applied Thermal Engineering.

Mahalingam, R. e Glezer, A., 2005, "Design And Thermal Characteristics Of A Synthetic Jet Ejector Heat Sink. Journal of electronic packaging", V. 127, N. 1, p. 172-177.

Malisca, C. R., 2004, "Transferencia de Calor e Mecanica dos Fluidos Computacional", Ed. LTC.

Smith, B. L. e Glezer, A., 1998, "The Formation and Evolution of Synthetic Jets", Physics of Fluids, V. 10, N. 9, p. 2281-2297.

Ohadi, M., 2010, "Thermal Management of Next Generation Low Volume Complex Electronics. Scottsdale", Az. CALCE, p.03-14.

Tang, H. e Zhong, S., 2009, "Lumped Element Modeling of Synthetic Jet Actuators", Aerospace Science and Technology, V. 13, N. 6, p. 331-339.

Wang, J., Shan, R., Zhang, C. e Feng, L., 2010, "Experimental Investigation of a Novel Two-Dimensional Synthetic Jet", European Journal of Mechanics – b/fluids, V. 29, N. 5, p. 342-350.

White, F., 1991, Viscous Fluid Flow 2a ed, McGraw Hill.

Williams R., Lee, J., Sam, H. e Mahalingan R., 2007, "Synthetic Jets for Forced Air Coolling of Eletronics", Magazine Eletricscooling, 23 Abr. 2007, <http://www.electronics-cooling.com/2007/05/synthetic-jets-for-forced-air-coolingof-electronics/>.

Xu, G. P., Tou, K. W. e Tso, C. P., "Numeral Modeling of Turbulent Heat Transfer from Discrete Heat Sources in Liquis-Cooled Channel", International Journal Heat and Mass Transfer, V. 41, N. 10, p. 1157-1166.

8. RESPONSIBILITY NOTICE